

Heat Capacities of Submonolayer He<sup>3</sup> and He<sup>4</sup> Adsorbed on Ar-Plated Copper\*

G. A. Stewart and J. G. Dash

*Department of Physics, University of Washington, Seattle, Washington 98105*

(Received 30 March 1970)

Extending the earlier study by Goodstein, McCormick, and Dash, we have measured the heat capacities of He<sup>3</sup> and He<sup>4</sup> films adsorbed in Ar-plated copper, at coverages  $x$  ranging from 0.1 to 0.8 monolayer from 0.5 to 4.2 °K. The broad features of the results include the following:  $C(T)$  for He<sup>4</sup> resembles the temperature dependence of two-dimensional Debye solids, but with characteristic temperatures  $\Theta_D$  which decrease as  $T$  falls;  $\Theta_D$  at high coverage agrees with the value 28 °K obtained by Goodstein *et al.*;  $\Theta_D$  decreases at lower  $x$ , but is surprisingly large (16 °K) at  $x=0.1$ ; He<sup>3</sup> heat capacities at high coverage are quite similar to He<sup>4</sup> films at the same areal density; at intermediate and lower coverages,  $C(x, T)$  of He<sup>3</sup> is significantly different from that of He<sup>4</sup> and displays a small peak or offset at  $T \approx 2$  °K. The data are compared with several microscopic models: localized adsorption, two-dimensional gases, noninteracting particles in a two-dimensional tunneling band, and two-dimensional solids. Each is shown to be inadequate to account for the observed variations with  $T$ ,  $x$ , and isotopic mass. The data are then compared with the behavior of a two-phase film, and this is found to agree with the data on He<sup>4</sup> over a substantial range of  $x$ , but it fails at low  $x$ . We are forced, by general arguments, to invoke surface inhomogeneity to resolve the paradox, and we examine an *ad hoc* model (due to Peierls) of a substrate consisting of two distinct regions, on which the helium is clustered into dense monolayer patches. The two-patch model is quite successful for He<sup>4</sup>, yielding two-dimensional characteristic temperatures  $\Theta_1=16$  °K,  $\Theta_2=28$  °K for the two species, the  $\Theta_D$  values and the areas belonging to each fraction of the substrate being practically independent of  $T$ . Agreement with the two-patch model implies that much of the substrate is substantially bare of adatoms, and hence that adatoms are strongly bound in the dense surface phases. The latent heat for two-dimensional vaporization is estimated to be at least 15°. This value is about 8° greater than the heat of vaporization of bulk liquid He<sup>4</sup>, implying a large enhancement due to interactions with the substrate. We propose a possible mechanism for the enhancement; namely, a local depression of the surface by the adatoms: a "mattress effect." The two-patch model is successful in describing  $C(T)$  for He<sup>3</sup> at high coverage, but  $C(T)$  at low coverage and the  $x$  dependence over the entire range shows that He<sup>3</sup> is significantly different from He<sup>4</sup>, but we have no explanation for the difference.

## I. INTRODUCTION

The heat capacities of adsorbed monolayers of He<sup>3</sup> and He<sup>4</sup> have  $T^2$  temperature dependences at low temperatures.<sup>1-4</sup> This simple trend, which has been found for films adsorbed on a variety of solid substrates, is taken as evidence that the dominant thermal excitations are phononlike, with spectral densities corresponding to two-dimensional Debye solids. Further evidence for phonon excitations has been adduced from the variations of the characteristic temperature  $\Theta_D$  with isotopic mass; the  $\Theta_D$ 's for He<sup>3</sup> and He<sup>4</sup> monolayers at high coverage being in the ratio of the square root of the inverse isotopic masses.<sup>3,4</sup>

It is only for "nearly completed" monolayers that the heat capacities have  $T^2$  dependences. Partial monolayers have been studied on one type of adsorption substrate, Ar-plated Cu.<sup>3,4</sup> It was found that a decrease in average coverage caused the heat capacity per He atom to increase and the temperature dependence to become much more complicated, tending to become linear in  $T$  at low

temperature. For one intermediate coverage of He<sup>4</sup>, the heat capacity displayed a broad maximum at  $T \approx 3$  °K. It was suggested that the broad maximum might indicate a diffuse melting transition between two phases in equilibrium on the surface, and that the linear terms in  $T$  might correspond to two-dimensional quantum gases at very low temperatures.

The present study was designed to explore the submonolayer region in greater detail, with a view toward testing the hypotheses of surface phase equilibrium, quantum degeneracy, and the detailed predictions of recent theories of quantum monolayers.<sup>5-9</sup> The study was made by comparing pairs of samples of pure He<sup>3</sup> and He<sup>4</sup> at virtually identical coverages in order to isolate the possible variations due to isotopic mass. Coverages ranged from about 0.1-0.8 monolayer, and temperature from 0.5 to 4.2 °K.

## II. EXPERIMENTAL DETAILS

Heat capacities were measured using a copper

calorimeter consisting of compressed and sintered powder<sup>10</sup> in a cylinder 2.5 in. long by 0.72 in. o.d. with 0.030-in. walls. The powder<sup>11</sup> was in the shape of flakes approximately 3- $\mu$  characteristic lateral dimension,  $\frac{1}{3}$ - $\mu$  thickness, and was forced into the cylinder using a hand press and die. After sintering, a  $\frac{1}{8}$ -in. hole was drilled through the resulting sponge to reduce equilibrium times during filling and a copper cap containing a  $\frac{1}{16}$ -in.-o.d. capillary tube was silver soldered to the capsule. Silver soldering was accomplished with the lower portion of the capsule immersed in a water bath to prevent excess sintering and oxidation. The interior surfaces of the calorimeter were reduced by heating in pure H<sub>2</sub> after soldering. A heater consisting of 100  $\Omega$  of manganin wire was wound on the outside of the calorimeter and bonded to the surface with GE 7031 varnish.

Surface-capacity measurements and calorimeter charging were performed at 77 °K. Bennet-Emmet-Teller (BET) argon and nitrogen isotherms yielded monolayer coverages of 13.2 and 12.6 cm<sup>3</sup> STP, respectively. The calorimeter was charged with a mixture of helium and argon, the argon in each case consisting of 1.2 BET monolayer equivalent. Gas quantities were measured to within 2%. The calorimeter was sealed by pinching the copper capillary tube and tinning the tip with soft solder. Since the end of the capillary had to be cut off each time the calorimeter was opened and readied for a new sample, the total mass of the calorimeter was slightly reduced. We included this correction to the heat-capacity data. Each experimental run involved the slow cooling of the calorimeter in order to ensure that the argon plated the substrate before any appreciable amount of He was adsorbed.

Calorimeter support was provided by a  $\frac{1}{8}$ -in. nylon rod extending upward from a 26-g chrome potassium-alum salt pill used for adiabatic demagnetization. The salt was hung in a micarta cylinder at the bottom of a 1-in.-o.d. brass sample chamber. This configuration is similar to previous work<sup>4</sup> except for the replacement of a superconducting heat switch by the nylon support rod and the absence of a mechanical support at the top of the calorimeter. Temperatures above 1.2 °K were achieved using a pumped bath with exchange gas, and calorimeter temperatures below 1.2 °K were obtained by cooling toward the salt-pill temperature through the weak thermal link provided by the nylon rod. Cooling times from 1.2 to 0.5 °K were approximately 5 h.

Carbon resistance thermometry was used for all heat-capacity measurements. A 56- $\Omega$  Allen-Bradley  $\frac{1}{2}$ -W resistor was used for temperatures above 2 °K and a less sensitive 100- $\Omega$  Speer for temperatures between 0.5 and 2 °K. Minimum

power dissipation in the sensor is 10<sup>-12</sup> W; there was no evidence of heating in the thermometers at the experimental power levels. Both thermometers were calibrated against the bath vapor pressure at temperatures above the pumping limit (~1.17 °K) and against the salt susceptibility for lower temperatures. Resistance calibration data is stored in a SPLINE<sup>12</sup> computer routine on a point-by-point basis; the resultant "fit" is equivalent to a function which yields continuity of the function and first two derivatives at each point of the input  $R(T)$  data.

Heat-capacity measurements over the interval 0.5–4.2 °K were performed using a pulse method with heater powers ranging from 3 to 300  $\mu$ W. The off-balance signal was monitored on a 10-in. chart recorder and the drift rate extrapolated in the conventional fashion to determine the temperature excursion. The timing clock counts in units of  $\frac{1}{120}$  sec and was synchronized with 60-Hz mains. Heating times ranged from 4 to 18 sec with about 6 sec the mean time. No dependence of heat capacity on pulse length was observed for these durations; this observation was taken as an indication of rapid equilibrium times in the substrate and film when compared to heating times. The heat-capacity points for temperatures below 2.0 °K were taken ascending in temperature as the calorimeter was heated from its minimum initial temperature subsequent to a demagnetization.

The film heat capacity was determined by subtracting the heat capacity of the calorimeter without helium from the total measured heat capacity with helium charge. The heat capacity of the helium-free calorimeter was stored in another SPLINE routine; for each heat-capacity point corresponding to a charged calorimeter the background signal for the same temperature was subtracted off using SPLINE interpolation. Heat capacities without helium film ranged from 1 to 10 mJ/°K in the interval 0.8–4.2 °K, and film signals for various measured helium coverages neglecting desorption effects ranged from 3 to 25% of the total signal over the same interval.

Substantial uncertainties may arise in the subtracted film signals when the percentage contribution to the total signal is small. We estimate the mean scatter in measuring the total heat capacity on typical runs at 0.7%. The deviation in the subtracted film signal corresponding to 0.7% uncorrelated uncertainty in the charged and uncharged calorimeter is

$$\frac{\Delta C_{\text{film}}}{C_{\text{film}}} = \frac{\sqrt{2}}{\alpha} \left( \frac{\Delta C}{C} \right)_{\text{total}} = \frac{0.99}{\alpha} \% , \quad (1)$$

where  $\alpha$  is the fractional film contribution to the total measured signal. The hyperbolic character

of Eq. (1) indicates the significant uncertainty in a subtracted result for sufficiently small film signals. At all coverages this statistical scatter masked other sources of uncertainty in the measurements. The estimated uncertainties in the data of Sec. II were determined using Eq. (1).

Table I lists the coverages and mean interatomic separations of all samples. The fractional monolayer coverage in all cases is defined by the number ratio of adsorbed He atoms to Ar atoms in a BET monolayer ( $13.2 \text{ cm}^2 \text{ STP}$ ) at  $77^\circ \text{K}$ .

Figures 1–5 present the basic heat-capacity data of the study as a function of temperature.  $\text{He}^4$  heat capacities are shown in Figs. 1 and 2 for four coverages in the interval 0.11–0.72 monolayer, and  $\text{He}^3$  data extend in five coverages 0.11–0.88 monolayer in Figs. 3–5. Surface coverages in the four corresponding runs for both isotopes at 0.72 monolayer and below agree to within 1.5%. For Figs. 1(a) and 3(a), the data are the contribution to the total measured heat capacity of He atoms comprising 50 ppm of the calorimeter system. The data are compared with theoretical curves for two-dimensional Debye solids having temperature-independent characteristic temperatures  $\Theta_D$  which best fit the regions  $T \gtrsim 2.5^\circ \text{K}$ . Detailed analysis in terms of the Debye and other models is postponed to later sections of the paper.

### III. PRELIMINARY ANALYSIS: MODELS OF HOMOGENEOUS MONOLAYERS

In this section, we compare the experimental results with the predictions of several simple models of homogeneous systems: localized monolayers, two-dimensional gases, two-dimensional band theory, and two-dimensional solids.

TABLE I. Experimental samples, coverages,<sup>a</sup> and mean interatomic spacings.<sup>b</sup>

Film No.	$N(\text{cc STP})$ ( $\text{He}^4$ )	$x$	$d_1(\text{Å})$	$d_2(\text{Å})$
112	1.45	0.11	11.0	11.9
113	4.11	0.31	6.5	7.0
115	6.85	0.52	5.0	5.4
117	9.51	0.72	4.3	4.6
107	1.45	0.11	11.0	11.9
108	4.13	0.31	6.5	7.0
109	6.98	0.53	5.0	5.4
114	9.45	0.72	4.3	4.6
116	11.56	0.88	3.9	4.2

<sup>a</sup>Fractional coverages  $x$  are computed as the ratio of  $N$  in the sample to the number of Ar atoms in 1 BET monolayer at  $77^\circ \text{K}$ .

<sup>b</sup>Interatomic spacings calculated from adsorption areas corresponding to  $N_2$  molecular areas of  $13.8 \text{ Å}^2 \times (d_1)$  or  $16.2 \text{ Å}^2 (d_2)$  (see Ref. 4).

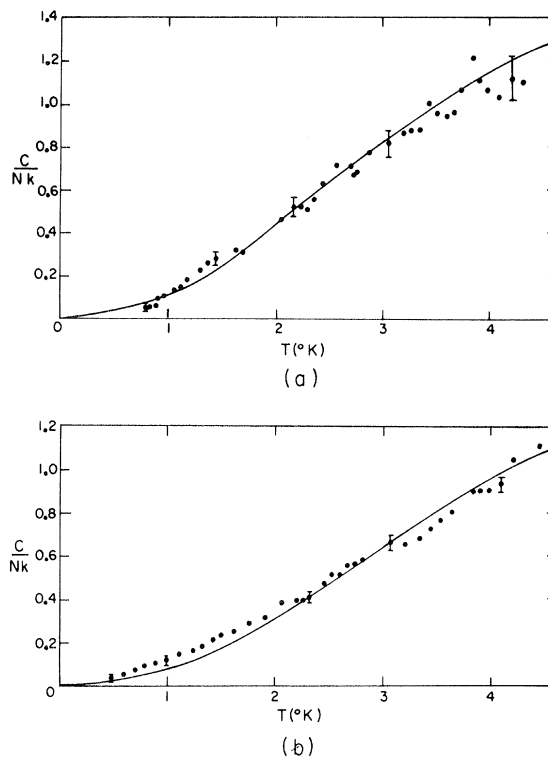


FIG. 1. Heat capacity of the  $\text{He}^4$  films of lowest coverages; (a)  $x=0.1$ ,  $\Theta_D=16^\circ$ ; (b)  $x=0.3$ ,  $\Theta_D=19^\circ$ .

#### A. Localized Monolayers

Previously measured heat capacities of helium monolayers have been compared with the behavior of localized monolayers<sup>4–6</sup> and have been shown to be at variance with the qualitative and quantitative character of localized adsorption. Here we give a brief review of the arguments, in the context of the present data.

The primary characteristics of localized monolayers, i. e., films composed of atoms bound to definite surface sites, are exponential heat capacities at low temperatures. For any site potentials, the localized single-particle excitation spectrum at low energies must have finite-energy-level separations  $\Delta \sim (\pi \hbar)^2/md$ , where  $d$  is the “size” of the site. At temperatures  $T \lesssim \Delta/k$ , the population of the first-excited level decreases exponentially with  $T$ , as  $\exp(-\Delta/kT)$ , and hence the heat capacity is modulated by the same exponential factor. In the presence of interactions between particles on neighboring sites, the single-particle levels will depend upon the state of excitation of the other particles. These interactions introduce a set of collective excitations in place of the discrete levels. However, the energy spectrum of the film will retain an energy gap between the ground state and the ex-

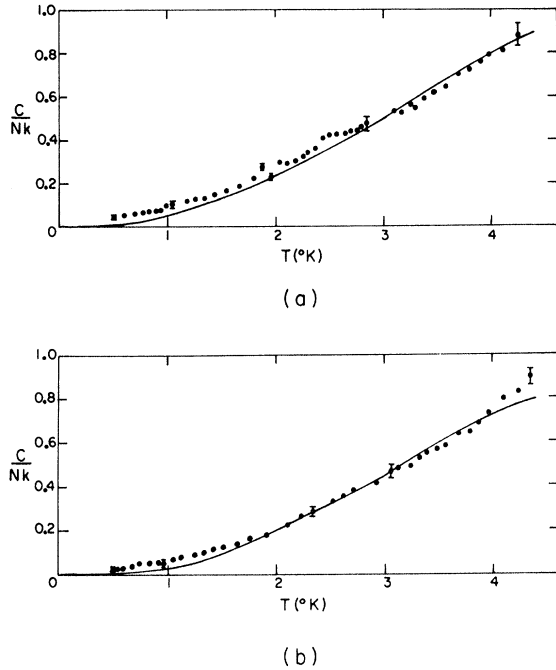


FIG. 2. Heat capacity of  $\text{He}^4$  films at intermediate coverages; (a)  $x=0.5$ ,  $\Theta_D=22^\circ$ ; (b)  $x=0.7$ ,  $\Theta_D=23.5^\circ$ .

cited states.<sup>7</sup> For  $\text{He}^4$  atoms localized on sites of  $d=2A$ , the quantity  $\Delta/k \sim 30^\circ\text{K}$ . Therefore, the signature of a localized He film at  $T=4^\circ\text{K}$  and below will be heat capacities much smaller than  $k$  per atom, decreasing exponentially at lower temperatures.<sup>13</sup>

The experimental results, showing heat capacities as high as  $k/\text{atom}$  at  $T \gtrsim 2^\circ\text{K}$ , varying with temperature as low powers of  $T$  down to  $0.5^\circ\text{K}$ , are taken as strong evidence for nonlocalization by substrate potentials. The absence of a definite dependence on isotopic mass, at least over a portion of the experimental range (see Sec. IIID), is additional indication of nonlocalization. The quantized energy levels of particles localized in square wells have separations  $m^{-1}$ ; harmonic wells have  $m^{-1/2}$ , and it can be shown that there are no single-particle potentials which yield mass-independent energy gaps.<sup>14</sup>

### B. Two-Dimensional Gases

Since localization is contraindicated, it is natural to compare the results with the opposite extreme model: a two-dimensional gas of atoms which are tightly bound to the substrate, but freely mobile along the surface. In the classical regime the atomic heat capacity will have the equipartition value for two dimensions, i. e.,  $k/\text{atom}$ . We expect classical behavior when  $\rho\lambda^2 \ll 1$ , where  $\rho$  is

the areal density of particles and  $\lambda$  is the thermal wavelength. In the present studies we covered the range  $0.5 \lesssim \rho\lambda^2 \lesssim 10$ , and hence the appropriate theoretical models are those of partial and extreme quantum degeneracy.

In the low-temperature limit, ideal Fermi and Bose gases have heat capacities linear in  $T$ , and except for mass and nuclear spin factors, they are identical in magnitude<sup>15</sup>:

$$C = (2\pi^3 g_n m A k^2 / 3h^2) T, \quad (2)$$

where  $g_n$  is the statistical factor for nuclear spin. The experimental results in the region of linear heat capacities are considerably lower than those predicted by Eq. (2) for the experimental coverages; if the masses  $m$  are treated as empirical parameters, then the experiments imply effective masses  $\approx \frac{1}{30}$  of the free-particle masses. This discrepancy cannot be accounted for by particle interactions, which will generally increase  $m^*$  above  $m$  of free particles. Another contradiction is seen in the dependence of  $C$  on coverage: Eq. (2) predicts total heat capacities independent of the total number of atoms in the sample, whereas the experimental heat capacities are strongly  $N$  dependent. Furthermore, the experimental heat capacities at low coverage appear to exceed the

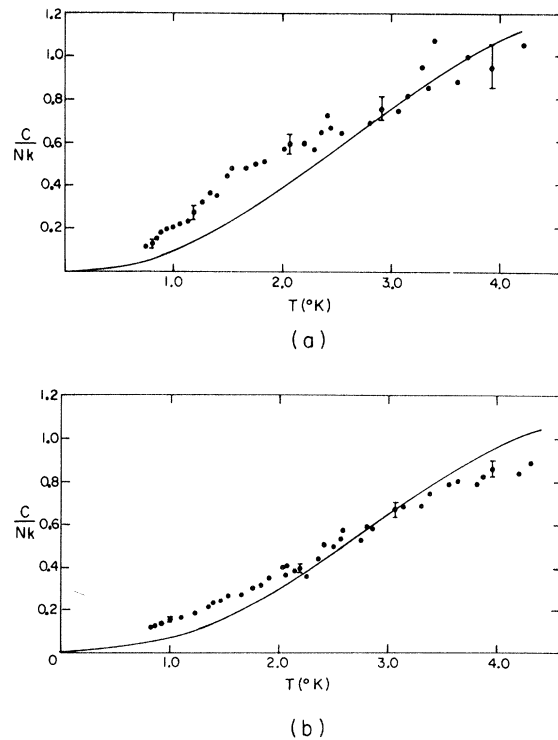


FIG. 3. Heat capacity of the  $\text{He}^3$  films of lowest coverages; (a)  $x=0.1$ ,  $\Theta_D=17^\circ$ ; (b)  $x=0.3$ ,  $\Theta_D=19^\circ$ .

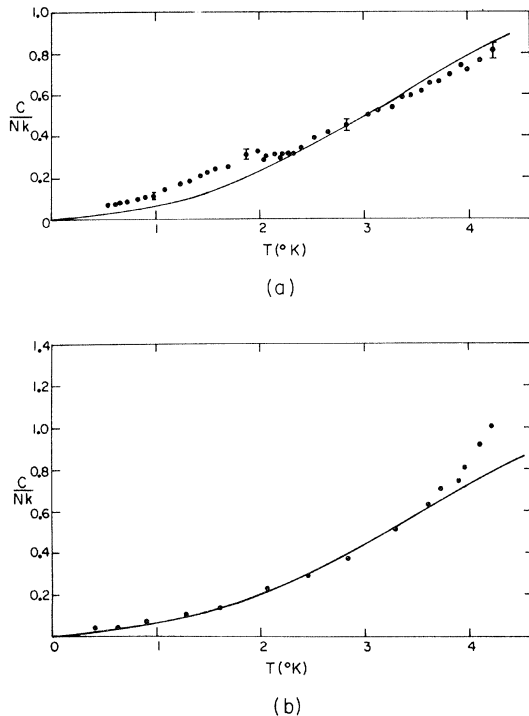


FIG. 4. Heat capacities of  $\text{He}^3$  films at intermediate coverages; (a)  $x=0.5$ ,  $\Theta_D=22^\circ$ ; (b)  $x=0.7$ ,  $\Theta_D=23.5^\circ$ .

classical value above  $3^\circ\text{K}$ .

### C. Band Theory

The quantum-mechanical theory of adsorption<sup>6</sup> offers greater realism than the models of complete localization or perfect two-dimensional mobility. Tunneling of adatoms among the adsorption sites of a physical substrate causes the single-particle levels to broaden into bands of states: Depending on the rapidity of tunneling, the band structure will vary between the extremes of the localized and mobile models. In the intermediate regime of moderate tunneling times the lowest band has a finite width and is separated from higher "thermal" bands by a finite energy gap. Heat capacities of adatoms having such a spectrum show considerable modulation, with a peak in the region of  $kT$  less than the width of the lowest band, a minimum at  $kT$  comparable to the energy gap, and a second maximum at  $kT$  of the order of the lower limit of the thermal band. The detailed behavior of the heat capacity depends upon the surface structure and the shapes of the site potentials,<sup>8</sup> but the general effects outlined above still remain. Although calculations have been given only for the case of noninteracting adatoms, the presence of relatively weak interatomic forces will not change the general character of the band effects.

The observed heat capacities of  $\text{He}^4$  films are monotonic with  $T$  and thus show that there are no isolated bands or dense groups of energy states having widths or separations  $0.5^\circ-4^\circ$ . This indicates that the lowest band has a width  $\gtrsim 4^\circ$ , or that it lies well below the explored range. Qualitative arguments based upon earlier work<sup>4</sup> suggested the former alternative. Recently, Ricca *et al.*<sup>16</sup> have made detailed numerical calculations of the band parameters of  $\text{He}^4$  adsorbed on (100) surfaces of solid Kr and Xe. They find for the widths  $\delta$  of the lowest band and the gap  $\Delta$  between the lowest and first excited bands

$$\text{Kr: } \delta = 0.06^\circ, \quad \Delta = 38.6^\circ;$$

$$\text{Xe: } \delta = 4 \times 10^{-4}^\circ, \quad \Delta = 42.9^\circ.$$

These calculated bandwidths are much too small and the gaps much too large to correspond to the data. However, for a (100) surface of Ar one expects larger  $\delta$  and smaller  $\Delta$ . Furthermore, a close-packed (111) plane, which we believe corresponds more closely to the Ar surface in the experiments, should yield further increase in  $\delta$  and decrease in  $\Delta$ . Milford and Novaco,<sup>17</sup> and Lai, Woo, and Wu<sup>18</sup> are currently calculating the band parameters of the He-Ar system, and their preliminary results indicate considerably greater bandwidths than those obtained by Ricca *et al.* for Kr and Xe surfaces.

A possible experimental determination of the width of the lowest band could be made by extending the heat-capacity measurements to lower temperatures to search for a band peak. However, such a test could not be conclusive, since it could not be known whether a peak would be found at temperatures below those explored. A conclusive test can be based upon entropy considerations. If there is a peak in the heat capacity at low temper-

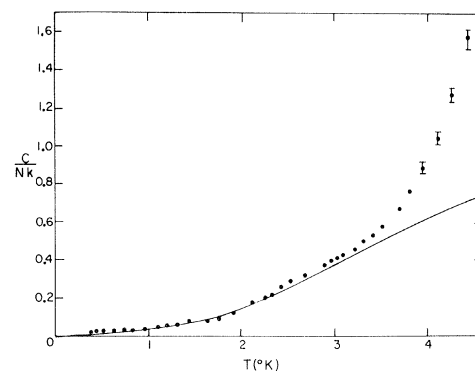


FIG. 5. Heat capacities of  $\text{He}^3$  at high coverage;  $x=0.9$ ,  $\Theta_D=26.2^\circ$ .

ature it will contribute to the total entropy at all higher  $T$ . Since the band theory requires as many states in each band as the number of adsorption sites on the surface, the band entropy must be at least  $k$ /atom for films of moderate coverage. If an experimental measurement of the total entropy were to yield a value well below  $k$ /atom, it would be proof of the absence of a large band peak at any lower  $T$ . Such a determination has been made<sup>19</sup> using a portion of the data acquired in this study: It is found that the total entropy in He<sup>3</sup> at 0.7 monolayer and  $T = 0.5$  °K is not greater than  $0.5k$ . This result, taken together with the absence of obvious band-structure effects in the heat capacity from 0.5 to 4 °K, leads to the conclusion that the lowest band has a width  $\gtrsim 4$ °. Although an entropy measurement has not been made for He<sup>4</sup> films or for He<sup>3</sup> films at coverages less than 0.7 monolayer, the similarities in temperature dependence of all samples indicates that this situation holds for all of the samples. We will present an analysis in Secs. V and VI indicating that the films are primarily composed of dense monolayer clusters. Since the theoretical calculations<sup>16-18</sup> are for isolated noninteracting atoms, their calculated bandwidths cannot be compared with our findings.

It is important to note that the absence of a significant amount of unresolved entropy shows that there cannot be a large number of low-lying excitations of *any character*, whether they be single-particle states or collective excitations of the entire film. Any energy spectrum possessing a large number of low-lying states will produce a heat capacity having a low-temperature peak at a value of  $kT$  comparable to the bandwidth, and its entropy contribution will remain saturated at all higher temperatures.

#### D. Two-Dimensional Solids

The  $T^2$  heat capacities seen in previous experiments have been taken as evidence that the films behave as two-dimensional Debye solids. However, while a theoretical two-dimensional Debye solid does have  $T^2$  heat capacity at small values of  $T/\Theta_D$ , it would be more correct to take the experimental  $T^2$  behavior as indicative of dense media having excitation spectra according to two-dimensional phase space, i. e., proportional to wave number.

Two recent theoretical studies have treated the collective excitations in He monolayers. Jackson<sup>9</sup> has a general theory of density fluctuations in a film adsorbed on a smooth substrate, and he shows that for He adsorbed on surfaces equivalent to monolayers of other noble gases plated on copper, the contributions of the transverse (surface-normal) modes to the heat capacity would be extremely

small at  $T < 4$  °K. Dash<sup>7</sup> studied the density fluctuations along the surface, treating the film as a monolayer of hard spheres adsorbed on a crystalline substrate, and showed that for rapid tunneling the heat capacity of longitudinal modes will have  $T^2$  temperature dependence.

Although  $T^2$  heat capacities do not prove that the Debye model is the correct description of He monolayers, the Debye formula nevertheless provides a convenient description of the heat capacity in terms of the single parameter  $\Theta_D$ . Therefore, we have analyzed the data to obtain the equivalent Debye temperature, using the complete two-dimensional Debye integral (assuming the same high-frequency cutoff for longitudinal and transverse vibrations) computed for various  $T/\Theta_D$ . As seen in Figs. 1-5, the data imply temperature-dependent  $\Theta_D$ 's. In Fig. 6, we show the empirical values  $\Theta_D(T)$  obtained by comparisons over large fractions of the density and temperature ranges of both isotopes. The general features of the dependence of  $\Theta_D$  on  $T$  and coverage are rather similar to the behavior of solid He. The magnitudes, lying between 15 and 25 °K, are comparable to the values of the *three-dimensional* characteristic temperatures of solid He<sup>3</sup> and He<sup>4</sup> at relatively low densities.<sup>20,21</sup> We find that  $\Theta_D$  changes appreciably

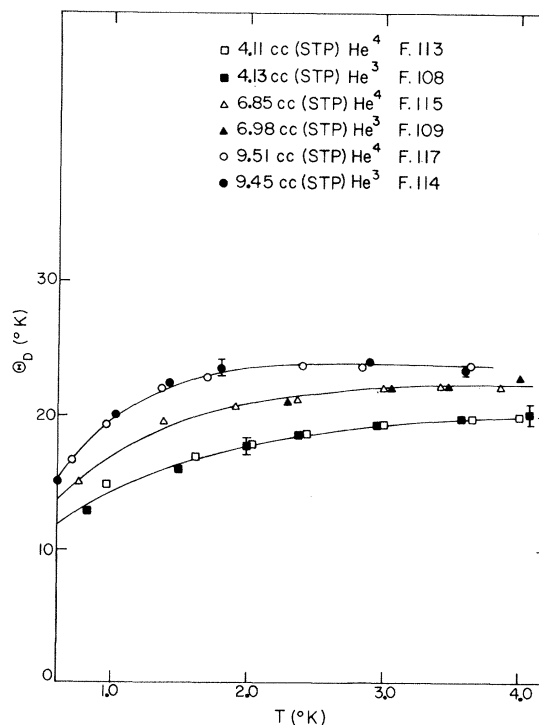


FIG. 6. Characteristic temperatures of He<sup>3</sup> and He<sup>4</sup> films for a portion of the data.

with  $T$ , exhibiting a low-temperature "softening" or decrease at lower temperatures. Similar softening has been seen for solid  $\text{He}^3$ .<sup>20</sup> The characteristic  $\Theta_D$  decreases with coverage, and this dependence is also analogous with bulk behavior. The dependence on isotopic mass is more surprising: According to the data in Fig. 6, there is no distinction between  $\text{He}^3$  and  $\text{He}^4$ . If there were no other data than the portion represented in Fig. 6, we would be motivated to search for mechanisms in which the absence of an isotope effect plays an important role in the fundamental nature of the film, and in fact, we were inclined in this direction during the preliminary analysis of the data. During that period we were impressed by the similar absence of isotopic dependence of  $\Theta_D$  in bulk solid He at low densities, where bcc  $\text{He}^3$  and hcp  $\text{He}^4$  of equal densities have the same characteristic temperatures.<sup>20</sup> However, two portions of the  $\text{He}^3$  data show heat capacities which are distinctly different from  $\text{He}^4$ .

One region in which the  $\text{He}^3$  and  $\text{He}^4$  data differ occurs at high coverage and high temperature. Comparison between  $\text{He}^4$  and  $\text{He}^3$  at  $9.45 \text{ cm}^3$  shows nearly identical heat capacities at  $T < 3^\circ\text{K}$  and monotonically diverging values above: We therefore expect that  $\text{He}^4$  and  $\text{He}^3$  at  $11.56 \text{ cm}^3$  would also diverge above  $3^\circ\text{K}$ . We believe the rapid rises of both samples of  $\text{He}^3$  above  $3^\circ\text{K}$  to be due to desorption to the vapor phase, and that the absence of such increases in  $\text{He}^4$  are due to a greater heat of adsorption for the heavier isotope. The temperature dependence of the "excess" heat capacity attributed to desorption has the exponential temperature dependence expected for this effect. The temperature dependence and magnitude of the excesses have been analyzed in a separate communication,<sup>19</sup> and the results of that analysis have been referred to in Sec. III C.

The second region in which  $\text{He}^3$  and  $\text{He}^4$  have different heat capacities is at  $T \lesssim 1.7^\circ\text{K}$ , at moderate and lower coverages. In a later section of this paper we present the data in a manner which demonstrates significant and qualitative differences between the two isotopes.

The magnitudes of  $\Theta_D$  approach those previously determined by Goodstein *et al.* for  $\text{He}^3$  and  $\text{He}^4$  films of slightly higher density and in view of the expected trend of  $\Theta_D$  with density, the differences are reasonable. The trend of  $\Theta_D$  with density is more carefully examined in Fig. 7, which presents the values of  $\Theta_D$  of  $\text{He}^4$  at "high"  $T (\gtrsim 2^\circ\text{K})$  versus the number of atoms in each sample. For comparison we also show the earlier values,<sup>3,4</sup> computing those coverages on the same basis as in our present scheme, described in Sec. II. The data fit a linear dependence of  $\Theta_D$  on  $N$ , implying a "two-

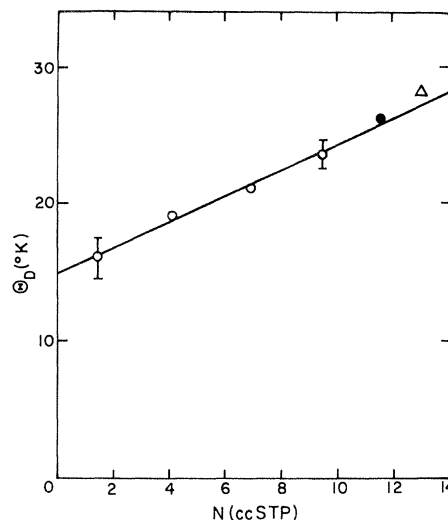


FIG. 7. Dependence of the empirical  $\Theta_D$  of  $\text{He}^4$  films ( $T \geq 2^\circ$ ) on the total quantity of sample.

dimensional Grüneisen constant"  $\gamma = -d(\ln\Theta_D)/d(\ln a) = 1$ , where  $a$  is the molecular area. If the empirical  $\Theta_D$ 's at high coverages are interpreted by means of the hard-sphere theory,<sup>7</sup> they imply adatom effective masses  $m^* \approx 1.7$  times the bare atomic masses, but the theoretical Grüneisen constant is considerably greater than unity at high coverage. A further and much more significant discrepancy is implied by the finite intercept of Fig. 7, because the theory predicts that  $\Theta_D \rightarrow 0$  linearly at low density. Furthermore, it is difficult to imagine any theoretical model for which  $\Theta_D$  should be as high as  $16^\circ\text{K}$  at the density of the  $1.45\text{-cm}^3$  film, for which the average interatomic distance is  $\sim 11 \text{ \AA}$ . At such large separations there should be negligible interaction between the He atoms, and if the tunneling of individual atoms between adsorption sites is as rapid as we have estimated, the monolayer should have a heat capacity resembling an ideal two-dimensional gas. Since the arguments previously given have eliminated localization and statistical degeneracy as responsible for the temperature dependence, they cannot now be invoked to explain the variations with coverage.

We now note that the argument above is based upon the assumption that the films have relatively uniform densities covering the entire substrate. If, however, the He tends to aggregate into two-dimensional clusters of high density, then the finite intercept of Fig. 7 can be understood as the characteristic temperature of the high-density clusters. This possibility can be put to a more stringent test by considering the thermodynamics of phase equilibrium, as in Sec. IV.

## IV. SURFACE PHASE EQUILIBRIUM

## A. Homogeneous Surfaces

If the adatoms tend to cluster into dense patches, then these clusters must be in equilibrium with atoms adsorbed on the remaining sparsely covered surface, i. e., with another surface phase of lower density. Equilibrium between the two surface phases and the vapor is characterized by the uniformity of the chemical potential throughout the sample. For an arbitrary displacement along the equilibrium line, the change in chemical potential of a surface phase is

$$d\mu_f = -s_f dT + v_f dP + ad\phi, \quad (3)$$

where  $\phi$  is the two-dimensional spreading pressure. For the vapor,

$$d\mu_v = -s_v dT + v_v dP. \quad (4)$$

Summing the contributions of surface phases 1, 2, and the vapor phase, the total sample of  $N$  atoms will obey the equilibrium relations

$$N \left( \frac{d\mu}{dT} \right)_{\text{eq}} = -S + V_0 \left( \frac{dP}{dT} \right)_{\text{eq}} + A \left( \frac{d\phi}{dT} \right)_{\text{eq}}, \quad (5)$$

$$N \left( \frac{d^2\mu}{dT^2} \right)_{\text{eq}} = \frac{-C}{T} + V_0 \left( \frac{d^2P}{dT^2} \right)_{\text{eq}} + A_0 \left( \frac{d^2\phi}{dT^2} \right)_{\text{eq}}, \quad (6)$$

where  $S$  and  $C$  are the total entropy and heat capacity of  $N$  atoms in the container of fixed  $V_0$ ,  $A_0$ . Since the equilibrium line is unique for all  $N$  in the two-phase region, the experimental heat capacity of a two-phase film will have the functional dependence

$$C_{\text{eq}}(N, T) = Nf(T) + g(T). \quad (7)$$

(6) is formally identical to the condition for equilibrium between two three-dimensional phases which was applied to the liquid-solid transition in  $\text{He}^3$ .<sup>22</sup> It should be noted that Eq. (7) is a necessary, but not sufficient, condition on phase equilibrium.

We can inspect the possibility of surface phase equilibrium in the experimental samples by plotting the total heat capacity versus  $N$ . The two isotopes will be discussed separately. The  $\text{He}^4$  data, shown in Fig. 8, do show linear-in- $N$  isotherms at all temperatures, for the three samples of coverage  $\alpha > 0.3$ , but the data for  $\alpha = 0.1$  definitely fall below the linear extrapolations. We may then tentatively identify the linear region as a domain of surface-phase equilibrium, and the low-coverage region with a single homogeneous phase. However, a further thermodynamic argument makes this picture unlikely. The temperature dependence of  $C_{\text{eq}}(N, T)$  has a distinctive

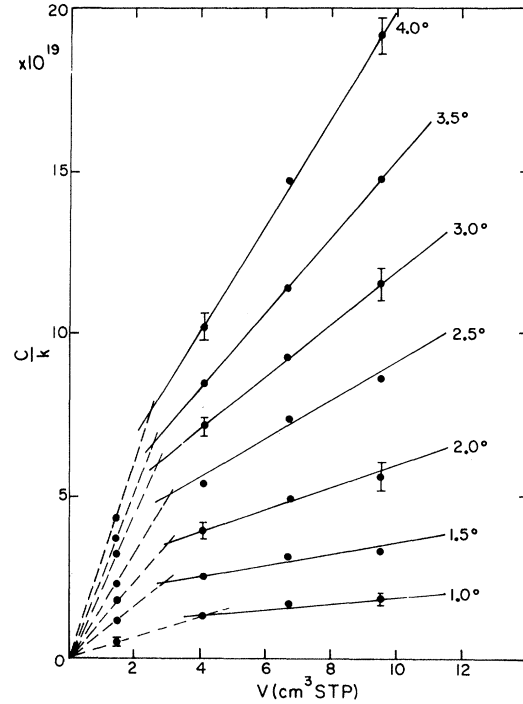


FIG. 8. The variation of heat capacity of  $\text{He}^4$  with quantity of sample.

signature at the boundary of a two-phase region, because of the disappearance of one of the phases, and such anomalies are not seen in the data. The thermodynamic proof is simple: If there are two coexisting phases (1, 2), the total entropy of a sample of fixed  $N = N_1 + N_2$  is

$$S(N, T) = S_1(T, N_1) + S_2(T, N_2), \quad (8)$$

and the equilibrium heat capacity is

$$C_{\text{eq}} = T \left( \frac{dS}{dT} \right)_{\text{eq}} = C_1 + C_2 + T \left[ \left( \frac{\partial S_1}{\partial N_1} \right)_T - \left( \frac{\partial S_2}{\partial N_2} \right)_T \right] \left( \frac{dN_1}{dT} \right)_{\text{eq}}, \quad (9)$$

where  $C_1$ ,  $C_2$  are the heat capacities of the pure phases at constant density. Upon crossing the two-phase boundary the third term disappears, producing a discontinuous change in the total heat capacity. No such discontinuities are seen at any temperature in any of the  $\text{He}^4$  samples.

The linearity in  $C_{\text{eq}}$  versus  $N$  over a portion of the  $T$  range, together with the absence of any singularities in the  $T$  dependence, can be due to special circumstances. Here we consider two hypotheses: (a) an "accidental" correspondence with Eq. (7) over a portion of the coverage range, the samples being composed of single homogeneous



phases throughout the region, (b) a nearby vertical phase boundary line, all three high-coverage samples being composed of two phases throughout the explored temperature region, and the lowest-coverage sample consisting of a single homogeneous phase in our experimental temperature range. Alternative (a), which presumes that Eq. (7) is satisfied by the simultaneous presence of different thermal excitations of special character, seems unlikely in view of the rather simple temperature dependence of the heat capacity. Although the Debye model is not strictly obeyed, the characteristic temperatures being  $T$  dependent, the over-all behavior is rather well described by the Debye model over a wide range of  $\Theta_D/T$ . We have previously discussed the characteristic signatures of other models, and have shown that they all disagree with either the coverage or the temperature dependence of the data. We therefore continue to believe that the films are basically two-dimensional solids. Since the  $N$  dependence of simple 2D solids does not obey Eq. (7), we reject hypothesis (a). Alternative (b) presents other difficulties. It implies that the two phases are *both* solidlike, since the phase persisting at low  $N$  has a Debye-like temperature dependence. This then restores one of the original difficulties in understanding the data; how a homogeneous phase at such low coverage can have solidlike excitations. Thus, the two-dimensional vapor phase, which was postulated in order to explain the large  $\Theta_D$  at low coverage, seems to have been eliminated by thermodynamic arguments.

A possible resolution of the dilemma arises when we relax an implicit constraint underlying all of the previous models, the assumption of a homogeneous substrate.

#### B. Phase Equilibrium on an Inhomogeneous Substrate

If we abandon the assumption of a uniform surface, the subsequent analysis can be based on a more realistic model of the substrate, for it is known that most real adsorbents have nonuniform surface properties due to cracks, impurities, and faceting.<sup>23</sup> A further advantage is that we gain much more latitude in parametrizing the data: Since atoms are preferentially adsorbed on regions of greater binding energy, it should be possible to represent any observed coverage dependence  $C(N)$  by means of an empirical distribution of binding energies. However, if the empirical distribution is also required to be independent of temperature, the combined dependence  $C(N, T)$  will, in principle, permit distinctions to be made among various microscopic models such as those discussed in Sec. III. We have not attempted an exhaustive

treatment of heat capacities on arbitrary inhomogeneous surfaces, but have analyzed the present results in terms of a simple *ad hoc* model which resolves the apparent inconsistencies of Sec. IV A.

The following model has been proposed by Peierls<sup>14</sup> after numerous discussions of the experimental results: (i) The surface is not uniform, but is composed of two types of homogeneous regions, each type having a characteristic binding energy for He adsorption. (ii) He adsorbed on each region of the surface tends to aggregate into dense monolayer patches resembling two-dimensional solids. The two species of dense patches have distinct characteristic Debye temperatures.

An adsorption isotherm on such a surface would show an intermediate step corresponding to the complete coverage of the preferential regions. The heat capacity of adsorbed He according to this model behaves according to

$$C(N, T) = NF_D(T/\Theta_1), \quad N < N_0; \quad (10)$$

$$C(N, T) = N_0F_D(T/\Theta_1) + (N - N_0)F_D(T/\Theta_2), \quad N > N_0; \quad (11)$$

where  $N_0$  is the capacity of the preferential patches and  $F_D$  is the two-dimensional Debye function.  $N_0$ ,  $\Theta_1$ , and  $\Theta_2$  are empirical parameters assumed to be constants over the experimental range of  $T$  and  $N$ .

We note that this two-patch model implies the possibility of five possible phases; vapor and two surface phases on each of the two types of homogeneous regions of the adsorbent. The dominant surface phases are assumed to be dense clusters, and hence, the remaining phase on each surface region must have low areal density. In a later section we will explore the effects of the low-density phases, but for the present we will merely assume that they contain so few atoms that they make no appreciable contributions to the heat capacity.

#### C. Two-Patch Model Applied to He<sup>4</sup>

The model implies that the data at low coverage define a family of straight lines in Fig. 8 which run from the origin to their intersections with the straight lines through the high-coverage data, and that the intersections are independent of  $T$ . We indeed find that the empirical values  $N_0$  are not strongly sensitive to  $T$ . The model also predicts that the empirical value of  $\Theta_D$  for the lowest coverage sample should be independent of  $T$ ; Fig. 9 shows this condition to be substantially obeyed. When we adopt this value as  $\Theta_1$  and the mean intersection position as  $N_0$ , the remaining parameter  $\Theta_2$  may be determined from the temperature dependence of the highest-coverage film. The set of

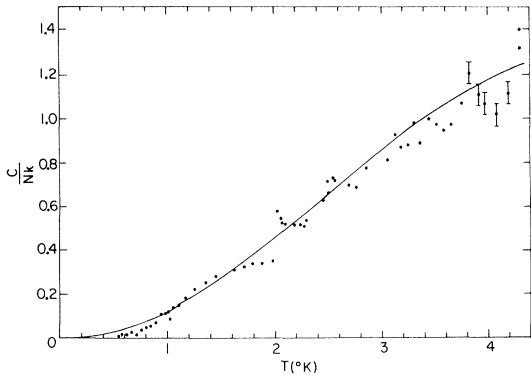


FIG. 9. Comparison of the two-patch model with the data for  $\text{He}^4$  at  $x=0.1$ ;  $\Theta_1=15.5^\circ$ .

empirical values found in this way is

$$\Theta_1 = 15.5 \pm 1 \text{ }^\circ\text{K}, \quad \Theta_2 = 28 \pm 2 \text{ }^\circ\text{K}, \quad N_0/N_m = 0.22 \pm 0.02,$$

where  $N_m$  is the Ar monolayer capacity (BET, 77  $^\circ\text{K}$ ). Although it may first seem that the three-parameter fit provides a high degree of flexibility in fitting the data, this is not at all the case. The three parameters are fixed for all  $T$  and  $N$ , and  $F_D$  is a universal Debye function. Nevertheless, the data for all of the  $\text{He}^4$  samples are described with fidelity; furthermore, we find that the quality of the fits is highly sensitive to rather small changes in the parameters. The curves given by Eqs. (10) and (11), with the best single set of parameters, are directly compared with the data in Figs. 9–12. There is, however, a tendency of the curves to fall below the data at low temperatures; the discrepancies are greatest for the intermediate coverages. They correspond to a small decrease in  $\Theta_1$  at low  $T$ . But the major decreases in  $\Theta_D$  at low  $T$  that had to be invoked in the homogeneous model (Fig. 6) are now absent; they are accounted for by the simultaneous presence at  $N > N_0$  of patches having markedly different  $\Theta_D$ 's.

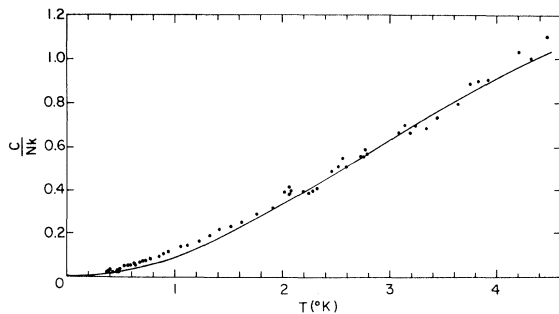


FIG. 10. Comparison of the two-patch model with the data for  $\text{He}^4$  at  $x=0.3$ .

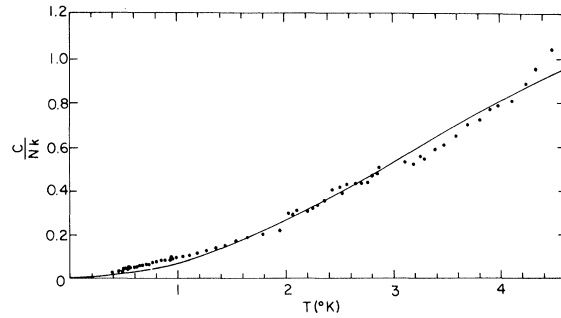


FIG. 11. Comparison of the two-patch model with the data for  $\text{He}^4$  at  $x=0.5$ .

#### D. Phase Equilibrium in Two-Patch Model: $\text{He}^4$

Agreement between the  $\text{He}^4$  and the two-patch model implies that virtually all of the adsorbed atoms are in high-density clusters. To the extent that we detect no heat-capacity contributions that must be attributed to phases other than two-dimensional solids, the remaining portions of the substrate cannot have many adsorbed atoms. Therefore, the cohesive energies of the solid phases must be rather large, and in this section we estimate a lower bound for the cohesion.

The total heat capacity of a two-phase film on a homogeneous substrate must be composed of three terms, as given by Eq. (9). Under the conditions of the model, the heat capacity of each condensed phase is given exactly by the theoretical Debye formula, and hence the presence of a low-density phase coexisting with a condensed phase should be evidenced by an excess heat capacity  $C'$ :

$$\begin{aligned} C' &= C_{\text{total}} - C_{\text{Debye}} \\ &= T \left[ \left( \frac{\partial S_g}{\partial N_g} \right)_T - \left( \frac{\partial S_D}{\partial N_D} \right)_T \right] \left( \frac{dN_g}{dT} \right)_{\text{eq}} + C_{g'}, \end{aligned} \quad (12)$$

where the subscript  $g$  refers to the low-density phase. Now we can obtain theoretical expressions

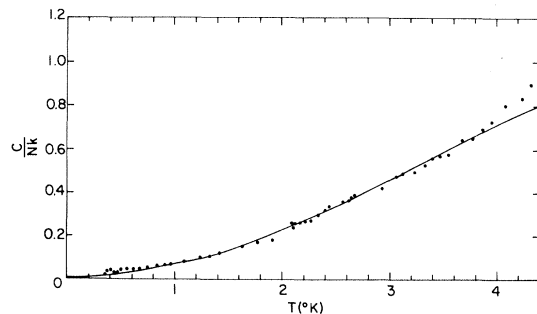


FIG. 12. Comparison of the two-patch model with the data for  $\text{He}^4$  at  $x=0.7$ .

for  $C'$  according to specific statistical models of the phases in equilibrium. For each solid phase, the Helmholtz free energy is, at  $T/\Theta_D \ll 1$ ,

$$F = -N\epsilon_0 + Nu(a) + \frac{2}{3}Nk\Theta_D - 4.808NkT(T/\Theta_D)^2, \quad (13)$$

where  $\epsilon_0$  is the binding energy between isolated adatoms and the substrate, and  $u(a)$  is the static energy per atom due to interactions with other adatoms. Our measurements give no clues as to the nature of the low-density phases, and hence, we will consider two extreme models; a localized monolayer and an ideal mobile two-dimensional gas. The free energies of these models, both assumed to be of very low density, are

$$F(\text{localized}) = -N\epsilon_0 - NkT \ln z + NkT \ln x, \quad (14)$$

$$F(\text{mobile}) = -N\epsilon_0 + NkT(\ln \rho \lambda^2 - 1), \quad (15)$$

where  $z$  is the single-site partition function and  $x = N/N_s$ , where  $N_s$  is the number of sites on the surface. We will assume the temperature to be so low that the localized adatoms are nearly all in their ground states so that  $z \cong 1$ .

The chemical potentials and entropies can be readily obtained from the expressions for  $F$ . Equating the chemical potential of the solid phase alternately to that of each model of the low-density phase, we obtain expressions for the number of atoms in the low-density phase:

$$N(\text{localized}) = N_s e^{-\epsilon_0/T}, \quad (16)$$

$$N(\text{mobile}) = A_g e^{-\epsilon_0/T} / \lambda^2, \quad (17)$$

where  $qk \equiv -u + a \left( \frac{du}{da} \right) - \frac{2}{3}(1+\gamma)k\Theta_D$ ,

the term involving  $(T/\Theta_D)^2$  having been neglected.  $a$  is the molecular area and  $\gamma$  is the two-dimensional Grüneisen constant as previously defined. The expressions for  $N$  and the entropies yield equations for the excess heat capacity according to Eq. (12):

$$C'(\text{localized}) = N_s k (q/T)^2 e^{-\epsilon_0/T}, \quad (18)$$

$$C'(\text{mobile}) = (A_g k / \lambda^2) [(q/T + 1)^2 + 1] e^{-\epsilon_0/T}. \quad (19)$$

In both of the above expressions, we have neglected the entropy of the solid phase.

We note that the excess heat capacity has the exponential temperature dependence expected for first-order phase transitions. By estimating the maximum amount of exponential character consistent with the measurements we can obtain an upper bound to  $C'$ , and with approximate values of the parameters, calculate lower bounds to  $q$  according to either model. A restriction on the use of these expressions is that they are appropriate only to homogeneous surfaces. According to the two-patch theory, the expressions for  $C'$  are applicable to a

film on a homogeneous surface, and hence according to the terms of the two-patch model, can be applied to the  $\text{He}^4$  sample of lowest coverage. We have no direct knowledge of the area of the preferential surface regions, but only its monolayer capacity  $N_0$ . If, however, we equate the fractional capacity  $N_0/N_m$ , which is equivalent to the assumption of equal densities in the two species of solid clusters, the resulting error in  $q$  is estimated to be no greater than 5%. The corresponding density of a cluster is  $6 \times 10^{14}$  atoms/cm<sup>2</sup>.

The quantities required for a calculation of  $q$  can now be estimated for the 1.45-cm<sup>3</sup>  $\text{He}^4$  sample: The area  $A_g$  and number of sites  $N_s$  available for the low-density phase on the preferential regions are  $A_g = 5 \times 10^4$  cm<sup>2</sup>;  $N_s = 4 \times 10^{19}$ .

We now require an estimate of the maximum value of  $C'$  consistent with the data: A conservative estimate is that  $C'$  is no greater than 20% of the total heat capacity of the sample. The corresponding lower bounds of  $q$  calculated at  $T = 1, 2,$  and  $3^\circ\text{K}$  are listed in Table II. It is fortunate that the calculation is not strongly dependent on the particular model of the low-density phase, the two extreme models yielding an average  $q \gtrsim 15.3^\circ$  at  $T = 3^\circ\text{K}$ . We also note that the value of  $q$  is not strongly dependent on the sensitivity criterion: A reduction of  $C'$  to 10% of the total heat capacity would increase the lower bound to  $18.3^\circ$ . Discussion of the implications of this estimate for  $q$  is postponed to the last section.

A more fundamental quantity than  $q$  is the static energy  $u(a)$ . The terms involving the unknown quantities  $\gamma$  and  $(du/da)$  can be eliminated from  $q$  by calculating the two-dimensional pressure  $\phi$  of the solid phase. From Eq. (13) we obtain the equation of state

$$\phi = - \left( \frac{\partial F}{\partial A} \right)_T = - \left( \frac{du}{da} \right) + \frac{2}{3} \frac{k\gamma\Theta_D}{a}. \quad (20)$$

Since the number of atoms in the low-density phase is proportional to  $\phi$ ,  $\phi \approx 0$ , and the resulting equation substituted in the expression for  $q$  then yields ( $q > 0, u < 0$ )

$$-u/k = q + \frac{2}{3}\Theta_D. \quad (21)$$

TABLE II. Lateral heat of adsorption of  $\text{He}^4$  on Ar-Cu.

Model	$T$ (°K)	Minimum $q$ (°K)
Two-dimensional mobile gas	1	8.1
	2	12.3
	3	15.2
Localized monolayer	1	7.9
	2	12.2
	3	15.3

Thus, we obtain  $u/k\zeta = -27^\circ$  corresponding to the 20% excess heat-capacity criterion and the Debye temperature  $\Theta_D = 16^\circ\text{K}$  for this sample. It is also clear from (21) and (13) that  $q$  is the increase in binding beyond the value  $\epsilon_0$  for isolated adatoms.

A calculation for the static energy of the solid patches with  $\Theta_D = 28^\circ\text{K}$  can in principle be carried out in the same manner. Such a calculation would be more uncertain due to the mixture of heat capacities of both species of solid phase: It appears, however, that it would yield values for  $u$  somewhat greater than the above.

Other quantities which would be important to know in order to test the consistency of the theory include the single adatom-substrate binding energies  $\epsilon_0$  for each species of surface patch. These quantities are difficult to obtain since they require measurements of vapor pressure at low coverage. However, there is one additional property which can be deduced at this time. According to the two-patch model, the preferential solid phase has the smaller value of  $\Theta_D$ , and the implications of this condition can be examined by considering the equilibrium between the two species of solid clusters.

If we imagine the course of a vapor-pressure isotherm in the model system, there would be two "vertical rises," the pressure remaining constant at some value  $p_A$  during the growth of the  $\Theta_D = 16^\circ$  species, and at some higher value  $p_B$  during the growth of the  $\Theta_D = 28^\circ$  species. The inequality  $p_B > p_A$  implies that the chemical potential of the  $\Theta_D = 16^\circ$  species must change between these two regions, such that

$$\frac{\partial q}{\partial p} < 0, \quad \text{when } p_A \leq p < p_B. \quad (22)$$

With the expression for  $q$  previously given and the equation of state Eq. (20), we obtain, after reduction,

$$a \left( \frac{\partial \phi}{\partial a} \right)_T \left( \frac{\partial a}{\partial p} \right)_T < 0. \quad (23)$$

The condition for mechanical stability requires  $(\partial \phi / \partial a)_T < 0$  and hence  $(\partial a / \partial p)_T < 0$ . Although contrary to the behavior of simple film models, this inequality does not appear inconsistent with any general conditions of thermodynamics; it must be kept in mind that the inequality refers only to the single phase characterized by  $\Theta_D = 16^\circ\text{K}$ , in the restricted pressure range between  $p_A$  and  $p_B$ .

#### E. He<sup>3</sup>

Following the lines of the He<sup>4</sup> analysis, we study the variation of He<sup>3</sup> heat capacity with coverage (see Fig. 13). The He<sup>3</sup> isotherms for  $T > 2.0^\circ\text{K}$  resemble those for He<sup>4</sup>, showing a linear region at moderate and high coverages, and apparent in-

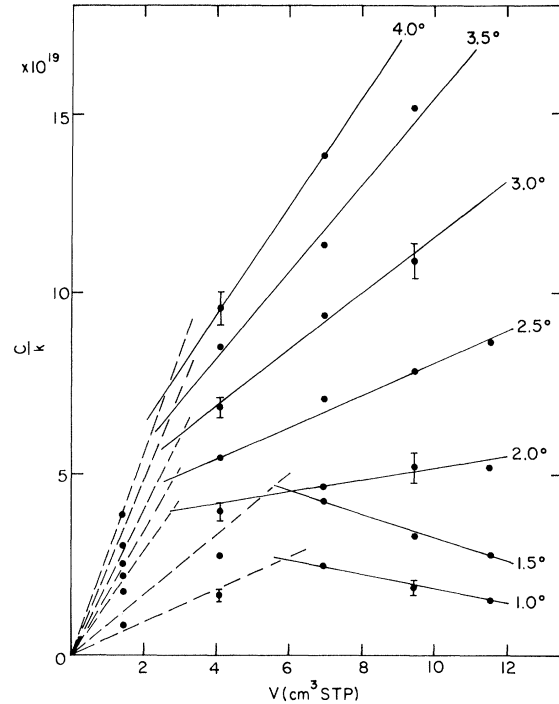


FIG. 13. Variation of heat capacity of He<sup>3</sup> with the quantity of sample.

tercepts with a low-coverage region at a comparable value of  $N_0$ . However, isotherms at lower  $T$  all show an additional feature, a region of negative slopes ( $dC/dN < 0$ ) for the three samples of highest coverage. It might be expected from direct examination of the  $T$  dependence of the heat capacities (Figs. 3–5) that the peak evident in the 6.98-cm<sup>3</sup> sample would produce some "anomalous" features in the isotherms. However, it had not been expected that the 9.51- and 11.56-cm<sup>3</sup> samples would show any anomalous behavior, since they have temperature variations which appear "normal." Yet we find in Fig. 13 that the slopes  $dC/dN$  are negative throughout the region of high coverage, and indeed, that the slope appears constant over the range  $N > 6$  cm<sup>3</sup>. The shape of the isotherm at low coverage does not permit us to identify an intersection as  $N_0$  for  $T < 2.0^\circ\text{K}$ : To explore this region we would need samples of closely-spaced coverages between 1 and 4 cm<sup>3</sup>.

We find another unexpected departure from the He<sup>4</sup> behavior when we try to apply the two-patch model [Eqs. (10) and (11)] to the He<sup>3</sup> sample of 1.45 cm<sup>3</sup>. The heat capacity does not follow a simple Debye law but instead shows a "transition" from one Debye function with  $\Theta_D = 12^\circ$  to one of  $\Theta_D = 18^\circ$  (Fig. 14). The transition from one characteristic temperature to the other is rel-

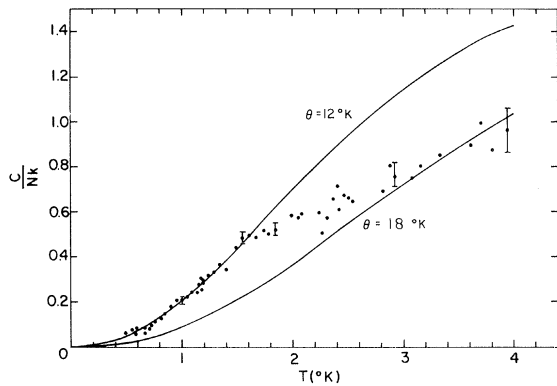


FIG. 14. Comparison of the two-patch model with the data for  $\text{He}^3$  at  $x=0.1$ .

actively abrupt, beginning rather suddenly at  $1.5^\circ\text{K}$ , and ending at about  $3^\circ\text{K}$ . If there had not been such close correspondence between the  $\text{He}^4$  sample and the Debye function, it would make little sense to analyze the  $\text{He}^3$  data in this way, but it now demonstrates a striking difference between the isotopes.

It now appears, from both Figs. 13 and 14 that, contrary to our preliminary analysis of characteristic temperatures (Fig. 6), there are substantial qualitative and quantitative differences between the heat capacities of the two isotopes. These differences are not apparent in the temperature dependences of the heat capacities at higher coverage: Indeed, we find that, except for the desorption contributions, the two-path model provides an excellent fit to these samples, with empirical parameters  $\Theta_1 = 16^\circ\text{K}$ ;  $\Theta_2 = 30^\circ$ ;  $N_0 = 3.0 \text{ cm}^3$ . We therefore consider the two-patch model as a convenient basis for a preliminary model of  $\text{He}^3$ , but these films need further study: At the present time we have no explanation of the region of negative slopes nor of the intermediate peaks in the heat capacity.

## V. DISCUSSION

The picture that emerges from this research, while retaining some broad features of the earlier work, is considerably more detailed. There is fairly conclusive evidence of phase equilibrium at  $4^\circ\text{K}$  and below, the dominant phases consisting of dense patches which behave as two-dimensional Debye-like solids. The variations of heat capacity with density and with temperature appear to show that the Ar-plated surface is inhomogeneous, being composed of two regions, on which the dense phases have markedly different characteristic temperatures. The lateral binding of each species of condensed phase is so large that there are no evidences for evaporation to low-density phases on

the remaining portions of the substrate, and we estimate that the lateral binding of the condensed phase of  $\text{He}^4$  on the preferential fraction of the substrate is at least  $15^\circ$ .

There are several points of divergence between the present results and those of the previous study on Ar-plated copper. In the earlier work, the two samples of highest coverages had heat capacities varying as  $T^2$  between  $0.5$  and  $3^\circ\text{K}$ , with characteristic temperatures of  $28 \pm 1^\circ\text{K}$  and  $31 \pm 1^\circ\text{K}$ , respectively. There were no perceptible linear terms in the heat capacity of these films, but both  $\text{He}^3$  and  $\text{He}^4$  at lower coverages showed marked linear contributions at  $T \leq 2^\circ$ . At a coverage of about  $0.5$  monolayer,  $\text{He}^4$  displayed a broad peak centered at about  $3^\circ\text{K}$ . It was suggested that the broad peak and the deviations from  $T^2$  behavior were indicative of two-phase equilibrium at low coverage, but no thermodynamic analysis was presented. We now have evidence in support of the conjecture of phase equilibrium, but, contrary to the earlier view that the two phases consisted of a two-dimensional solid and a liquid or gaseous phase, we find a coexistence of two phases with solidlike excitations.

We cannot resolve these discrepancies, but believe that some of them are associated with minor differences between the substrates. The first study was carried out on a slightly coarser sponge (MD60<sup>12</sup>) sintered at higher temperature ( $650^\circ\text{C}$ ) than that we used (MD90,  $450^\circ\text{C}$ ). An additional, and perhaps more important, difference might be due to the quantity of Ar plating. In both studies, this was fixed at  $1.2$  BET monolayer at  $77^\circ$ , but the precise location of "1 BET monolayer" is difficult to distinguish from vapor-pressure isotherms.

In the following paragraphs we venture some speculations on the nature of the inhomogeneity of the substrate and the origin of the strong lateral cohesion.

The two regions of the substrate have apparent monolayer capacities of about  $20$  and  $80\%$  of a completed monolayer of He at  $4^\circ\text{K}$ . The quantity of Ar plating in these studies was chosen to be  $1.2$  BET monolayers, in order to ensure that no bare Cu surface remained. The similarity in the magnitudes of the two fractions (representing the preferred area for He adsorption and the excess Ar beyond 1 BET monolayer) presents an intriguing possibility: If, contrary to expectations, the Ar plating is composed of large (compared to molecular areas) regions of 1- and 2- monolayer thicknesses, the distinct He "solids" could correspond to clusters on the single and double Ar regions. The patches must be of sufficient size to permit phonon excitations of moderately long wavelength, at least several hundred  $\text{\AA}$ . The pos-

sibility of stepwise monolayer formation of Ar is made more plausible by recalling that He is adsorbed in stepwise fashion on bare Au<sup>24</sup> and on Ar-plated Cu,<sup>4</sup> and that Ar vapor-pressure isotherms exhibit steps on Kr- and Xe-plated graphite.<sup>25</sup> This model implies that He is adsorbed preferentially on the regions of double Ar layers; although this is a surprising result, it does not appear to imply any violations of thermodynamics or inconsistencies with other aspects of the analysis. Our speculations can be tested by a study in which the Ar coverage is varied, and such experiments will be made in the near future.

The lateral binding of the condensed patches is substantially larger than can be expected from normal He-He interactions. If we estimate the normal interaction as comparable to that in liquid He<sup>4</sup> at low temperatures, then we must account for an additional attractive energy of at least 8°, which must evidently be due to an enhancement by the substrate. Here, we venture a hypothesis that the strong lateral binding derives from changes in the total attractive interaction with the adsorbent. Specifically, we imagine the adsorption surface to be slightly compressible, so that it is locally depressed in the neighborhood of a He adatom. This local deformation would increase

the single He-surface attraction. If the local distortion of the substrate extends for some distance around an adatom, then it would present to any other adatom a region of stronger adsorption energy. A similar "mattress effect" exists in several macroscopic systems, as, e.g., among particles floating on the surface of a liquid, as well as the obvious conubial analogy. Further experimental studies on different substrates should provide some important clues in testing the conjecture.

#### ACKNOWLEDGMENTS

We are extremely grateful to several colleagues and associates for advice, assistance, and suggestions made at various stages of this study. R. E. Peierls, through his critical and continuing interest, has contributed materially to the work. His suggestion of the three-parameter model made it possible to advance our analysis to its present development. At various stages we had useful discussions with F. J. Milford, R. D. Puff, M. Schick, and E. A. Stern, and their contributions are blended into many sections of the paper. J. Torode assisted with many of the measurements and much of the data reduction.

\*Research supported by the National Science Foundation.

<sup>1</sup>H. P. R. Frederickse, *Physica* **15**, 860 (1948).

<sup>2</sup>D. F. Brewer, A. J. Symonds, and A. L. Thompson, *Phys. Rev. Letters* **15**, 182 (1965).

<sup>3</sup>D. L. Goodstein, W. D. McCormick, and J. G. Dash, *Phys. Rev. Letters* **15**, 447 (1965); **15**, 740 (1965).

<sup>4</sup>W. D. McCormick, D. L. Goodstein, and J. G. Dash, *Phys. Rev.* **168**, 249 (1968).

<sup>5</sup>J. G. Dash, *J. Chem. Phys.* **48**, 2820 (1968).

<sup>6</sup>J. G. Dash and M. Bretz, *Phys. Rev.* **174**, 247 (1968).

<sup>7</sup>J. G. Dash, *J. Low Temp. Phys.* **1**, 173 (1969).

<sup>8</sup>M. Bretz, *Phys. Rev.* **184**, 162 (1969).

<sup>9</sup>H. W. Jackson, *Phys. Rev.* **180**, 184 (1969).

<sup>10</sup>D. L. Goodstein, W. D. McCormick, and J. G. Dash, *Cryogenics* **6**, 167 (1966).

<sup>11</sup>MD90 Druid Copper, Alcan Metal Powders, Inc., Elizabeth, N. J.

<sup>12</sup>R. H. Pennington, *Introductory Computer Methods and Numerical Analysis* (MacMillan, New York, 1965), Chap. XV; *Mathematical Methods for Digital Computers*, edited by A. Ralston and H. S. Wilf (Wiley, New York, 1967), Chap. 7.

<sup>13</sup>The arguments previously given in this paper and elsewhere (Ref. 7) for an exponential temperature dependence cause by site localization are essentially dependent on the assumption of negligible interaction between the adatoms. A more general argument for the case of interactions among localized adatoms has been constructed by C. E. Campbell and M. Schick

(private communication), as follows: In the presence of interactions between the adsorbed atoms, the excitation spectrum at zero wave number remains characterized by a gap  $\Delta$ . This is due to the fact that, unlike a bulk solid which may be translated uniformly without the expenditure of energy, uniform translation of a solid produced by substrate localization requires the displacement of each adsorbed atom within the potential well produced by the substrate, thus requiring an energy  $\Delta_0$  per particle. If the minimum of the excitation spectrum occurs at zero wave number, then the existence of such a gap can again be excluded by the current experimental data. There remains the possibility that the minimum of the excitation spectrum occurs at a nonzero momentum  $p_0$  in the vicinity of which the spectrum has the form  $\epsilon(p) = \Delta + c(p - p_0)^2$ . Assuming that the value of  $\Delta/k$  is substantially larger than the temperature of interest, one finds that the ratio of the heat capacity to entropy depends only on the parameter  $\Delta/kT$ . A fit of the experimental ratios yields the following. First,  $\Delta(T)/kT$  is larger than unity at all  $T$ , thereby justifying this initial assumption. Second,  $\Delta(T)$  decreases greatly with temperature throughout the range of the experimental data, indicating little correspondence between the system and the above model at the temperatures investigated. Last,  $\Delta(T)$  remains a decreasing function of  $T$  down to the lowest temperatures studied, where it attains a value of approximately 1°. Thus, it can be concluded that there is no experimental evidence for localization in preferential adsorption sites. However, the possibility

of such a phase characterized by an excitation spectrum with a minimum energy less than  $1^\circ$  at a nonzero wave number can not be excluded.

<sup>14</sup>R. E. Peierls (private communication).

<sup>15</sup>R. M. May, Phys. Rev. **135**, A1515 (1964).

<sup>16</sup>F. Ricca, C. Pisani, and E. Garrone, J. Chem. Phys. **51**, 4079 (1969).

<sup>17</sup>R. J. Milford (private communication).

<sup>18</sup>C. W. Woo (private communication).

<sup>19</sup>J. G. Dash, R. E. Peierls, and G. A. Stewart, Phys. Rev. A, following paper, **2**, 932 (1970).

<sup>20</sup>H. H. Sample and C. A. Swenson, Phys. Rev. **158**, 188 (1967).

<sup>21</sup>R. C. Pandorf and D. O. Edwards, Phys. Rev. **169**, 222 (1968).

<sup>22</sup>D. O. Edwards, A. S. McWilliams, and J. G. Daunt, Phys. Letters **1**, 101 (1962).

<sup>23</sup>D. M. Young and A. D. Crowell, *Physical Adsorption of Gases* (Butterworths, London, 1962), Chap. 7.

<sup>24</sup>L. Meyer, Phys. Rev. **103**, 1593 (1956).

<sup>25</sup>J. H. Singleton and G. D. Halsey, J. Phys. Chem. **58**, 330 (1954); **58**, 1011 (1954).

PHYSICAL REVIEW A

VOLUME 2, NUMBER 3

SEPTEMBER 1970

## Desorption, Vapor Pressure, and Absolute Entropy of Adsorbed Films: Application to He<sup>3</sup>†

J. G. Dash, R. E. Peierls,\* and G. A. Stewart

*Department of Physics, University of Washington, Seattle, Washington 98105*

The experimental heat capacities of physically adsorbed films are increased by contributions due to desorption to the vapor phase, and these contributions are usually treated as an experimental nuisance. If the desorption contributions can be isolated from the total heat capacity, the measurements can lead to a model-independent determination of the vapor pressure and heats of adsorption of the film. The theory is applied to recent results on He<sup>3</sup> monolayers. The vapor pressures and heats of adsorption deduced from desorption, together with the measured heat capacities, are used to estimate the absolute entropy of He<sup>3</sup> submonolayers at 0.5 °K.

### I. INTRODUCTION

Measurements of the heat capacity of adsorbed films are sometimes complicated by unwanted desorption effects which cause the coverage to be temperature dependent and the total heat capacity to increase above the isosteric value. The equilibrium heat capacity can be corrected to the isosteric value if there are ancillary pressure measurements on the same system. For many experimental systems, the measurement of vapor pressure is relatively simple, but in some cases it is subject to considerable uncertainty arising from large and variable thermomolecular pressure differences. Vapor pressures in themselves yield important information on the thermodynamics of adsorption: If both vapor pressures and heat capacities are known, they can be used to deduce the absolute entropy of the film.

A recent study of the heat capacity of He<sup>3</sup> and He<sup>4</sup> monolayers<sup>1</sup> disclosed exponential increases in the heat capacities of He<sup>3</sup> films at relatively high coverage and temperature, and these increases appeared to have the magnitude and temperature dependence predicted on the basis of simple models

of desorption. In this paper, we show that the desorption contribution can be related to the vapor pressure by purely thermodynamic considerations, i. e., without resorting to specific models. As a rough check on the technique, we carried out conventional pressure measurements on the same system.

There are certain obvious advantages to a single technique for obtaining heat capacities and vapor pressures on virtually identical specimens. The technique may be applicable to systems other than helium. In this paper we present the theory relating the vapor pressure to the desorption heat capacity, and we apply it to some recent results on He<sup>3</sup> monolayers.

The calculated pressures, together with the measured heat capacities of the film, provide the basis for a calculation of the excess entropy of the monolayers at  $T = 0.5^\circ\text{K}$ .

### II. THEORY

The condition for equilibrium between the gas and adsorbed film is<sup>2</sup>

$$\frac{\partial F_f}{\partial N_f} = \frac{\partial F_g}{\partial N_g}, \quad (1)$$